Debiased Coordinate Conversion of Bistatic Radar Measurements

Richard A. Coogle, L. Donnie Smith, and W. Dale Blair
Georgia Tech Research Institute
Atlanta, Georgia 30332–0250
Email: {rick.coogle, larry.smith, dale.blair}@gtri.gatech.edu

***Abstract*— The introduction of biases into monostatic radar measurements as a result of conversion from sine space coordinates into Cartesian coordinates is a well-known problem. Specifically, this problem occurs in long-range radars or radars with high range resolution. However, the biases have only been determined with regard to monostatic radars. With a possible resurgence in bistatic radar, specifically since in certain cases, a Multiple-Input-Multiple-Output (MIMO) radar system can be formulated in terms of bistatic radar pairs, understanding the biases as a result of such coordinate conversions becomes important. In this paper, we present the equations for transforming bistatic measurements into Cartesian coordinates, as well as derive expressions for the biases in the mean and covariance that result.**

I. Introduction

A challenging problem occurs when tracking targets at either a long range or with very high range resolution. Consider a measurement taken by the radar in the *r-u-v* sine space coordinates with the measurement errors Gaussian and non-correlated. When the measurement is converted into Cartesian coordinates, the resulting errors are no longer Gaussian. In fact, the error volume has the shape of a contact lens [1], which forms a three-dimensional shell, rather than ellipsoidal as in the Gaussian case. However, this shape is not typically preserved when this transformed measurement covariance is used in tracking; that is, linearization is used in order to approximate the errors in the measurements. In high range resolution or long-range cases, this linearization will not be appropriate to cover the errors, as the size of the error volume will tend to be smaller than what is required to achieve a desired probability of containment for Gaussian errors. As a result, the converted Cartesian measurements will have a bias.

Several researchers have addressed this issue in the *monostatic* radar case. There are two general formulations: additive and multiplicative biases. The primary work covering each is given in [2] and [3], respectively. Appropriate debiased covariance matrices were also derived in both cases. It should be noted that the volume covered by these covariance matrices is generally larger than that of the linearized covariances in order to properly cover the errors.

In the bistatic radar case, research addressing the biases has been largely absent. Willis, in his seminal text [4], characterizes the range and angle errors in the bistatic case and gives the derivations necessary to construct coordinate conversions in the two dimensional case, but he does not derive the biases. The case for performing such a derivation, as well as giving the appropriate constructions for the coordinate conversions, is stronger now, as a result of another resurgence of bistatic radar. Specifically, it can be stated that for certain formulations of the Multiple-Input-Multiple-Output (MIMO) radar problem, MIMO radar can be considered to be a special case of bistatic radar. That is, with the orthogonal waveform assumption, a MIMO radar system can be modeled as a set of bistatic pairs [5] [6].

This paper is organized as follows. In Section II, we present a short overview of the transformation from bistatic sine space coordinates to receiving-sensor-relative Cartesian coordinates. Section III gives the derivations of the associated biases and unbiased measurement covariance, while Section IV provides results of simulations of these equations. In Section V, we conclude the paper.

II. Bistatic Coordinate Conversion

In short, a bistatic radar system is a radar system where a transmitting radar illuminates a target, while a *different* receiving radar obtains and processes the returns. This is in contrast to monostatic radar where the transmitter and receiver are colocated. Bistatic radar range measurements R_b are thus defined to be the following:

$$R_b = R_T + R_R$$

where R_T is the range from the transmitter to the target, and R_R is the range from the target to the receiver.

The separation of the transmitter and receiver and the definition of bistatic range causes the *contour of constant range* about the radars to be an ellipse. The transmitter and receiver act as the foci of this ellipse [4]. Figure 1 gives an illustration of this phenomenon for a single target, in the two dimensional case. In monostatic radar, the contour of constant range is trivially a circle with the radar at the center. Angle measurements are taken with respect to the receiver which are given as the sine space u and v coordinates.

If we initially consider receiver range to be a function of R_b, we have the following for converting from sine space into

978-1-4673-0658-4/12/$31.00 ©2012 IEEE

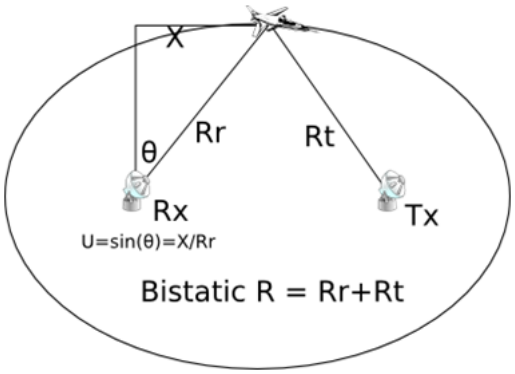

Fig. 1. Illustration of the bistatic ellipse for the two dimensional case, showing the relationship between sensor-face-relative Cartesian and polar coordinates.

Cartesian coordinates relative to the receiving radar's face[1]:

$$x = R_R(R_b, u, v) \cdot u$$
$$y = R_R(R_b, u, v) \cdot v$$
$$z = R_R(R_b, u, v) \cdot w$$

where $w = \sqrt{1 - u^2 - v^2}$. The complexity is in determining an equation for the receiver range that does not require explicit knowledge of the transmitter range and target position. We assume that the position of the transmitter is known. Next, we define target position to be the vector $\mathbf{x_T} = \begin{bmatrix} x & y & z \end{bmatrix}^T$, where the coordinates are defined to be as above.

We first define $\mathbf{z}$ to be

$$\mathbf{z} = \begin{bmatrix} u \\ v \\ w \end{bmatrix} \tag{1}$$

and the transmitter's known position *relative to the receiver* $\mathbf{x_{tx}}$ to be

$$\mathbf{x_{tx}} = \begin{bmatrix} x_{tx} \\ y_{tx} \\ z_{tx} \end{bmatrix} \tag{2}$$

We can then define a to be

$$a = \mathbf{z}^T \mathbf{x_{tx}} \tag{3}$$
$$= \left(\frac{1}{R_R} \mathbf{x_T}^T \right) \cdot \mathbf{x_{tx}} \tag{4}$$

which gives us the relationship we need to find the receiver range. We note that the transmitter range R_T is equal to[2]

$$R_T = \|\mathbf{x_T} - \mathbf{x_{tx}}\| \tag{5}$$

Hence, with some algebra, the receiver range may be found to be

$$R_R = \frac{R_b^2 - \|\mathbf{x_{tx}}\|^2}{2(R_b - a)} \tag{6}$$

[1]This means that we place the receiver at $(x, y, z) = (0, 0, 0)$ in the three-dimensional case, with the z coordinate positive outward from the radar face. Transforming from this sensor-relative frame to "world coordinates" is then a simple rotation and/or translation.

[2]$\|\cdot\|$ represents the Euclidean norm in this case.

All of the quantities in the resulting receiver range equation are either known or measured.

We may note the similarity between this equation and the special case of the receiver range for two dimensions and explicit sensor azimuth angles given in [4]:

$$R_R = \frac{R_b^2 - L^2}{2(R_b + L \sin\theta_R)}$$

L is defined to be the separation distance between the transmitter and receiver, and θ_R is the receiver's azimuth angle. It should be clear that $L = \|\mathbf{x_{tx}}\|$ and $\sin\theta_R = u$. That is, if our formulation is restricted to two dimensions and the transmitter and receiver lie on the x-axis:

$$a = u x_{tx} = u\|\mathbf{x_{tx}}\| = L \sin\theta_R$$

If we make the appropriate substitutions into our version of the receiver range, we will find a minus sign instead of a plus sign in the denominator. This is a result of the fact that, if we consider the two dimensional case, we assume the receiver to be in an effectively *negative* direction with respect to the transmitter: i.e. the positions of the transmitter and receiver are reversed in contrast to the geometry given in [4]. This changes the sign of the azimuth angle, and hence the sign in the denominator.

From these conversions, a Jacobian may be derived in order to transform a bistatic *r-u-v* measurement covariance $\mathbf{R_{ruv}}$ into a Cartesian measurement covariance $\mathbf{R_{xyz}}$. That is, for measurements of the form,

$$\mathbf{z_{ruv}} = \begin{bmatrix} R_b \\ u \\ v \end{bmatrix}$$

we can transform the associated measurement covariance $\mathbf{R_{ruv}}$ using the equation

$$\mathbf{R_{xyz}} = \mathbf{J}\mathbf{R_{ruv}}\mathbf{J}^T$$

where the Jacobian $\mathbf{J}$ is defined to be

$$\mathbf{J} = \begin{bmatrix} \frac{\partial x}{\partial R_b} & \frac{\partial x}{\partial u} & \frac{\partial x}{\partial v} \\ \frac{\partial y}{\partial R_b} & \frac{\partial y}{\partial u} & \frac{\partial y}{\partial v} \\ \frac{\partial z}{\partial R_b} & \frac{\partial z}{\partial u} & \frac{\partial z}{\partial v} \end{bmatrix}$$

This essentially converts the error volume to an ellipsoid, as shown in Figure 2.

If we draw samples representing *r-u-v* measurements from a multivariate Gaussian distribution and transform the samples into Cartesian coordinates, we will find that the distribution of the transformed measurements appears to bend along the contour of constant bistatic range. If we draw a containment region around the samples, it appears very similar to a bent covariance ellipse. This phenomenon is shown in Figure 3, with additional detail in Figure 4. This suggests that the errors are not jointly Gaussian in this case. In fact, if we use the Jacobian for the Cartesian coordinate transform in order to linearize the covariance of the original Gaussian distribution used to generate the samples, the resulting ellipsoid will not provide sufficient containment to cover all of the errors. That

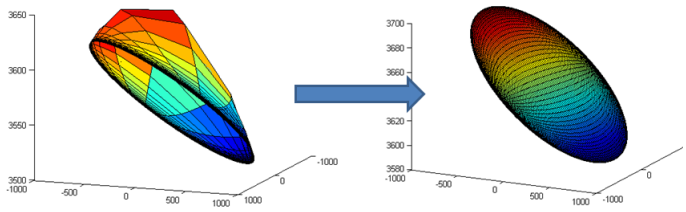

Fig. 2. Illustration of the error volume for a bistatic measurement, converted to an ellipsoid by linearization via the Jacobian of the Cartesian transformation.

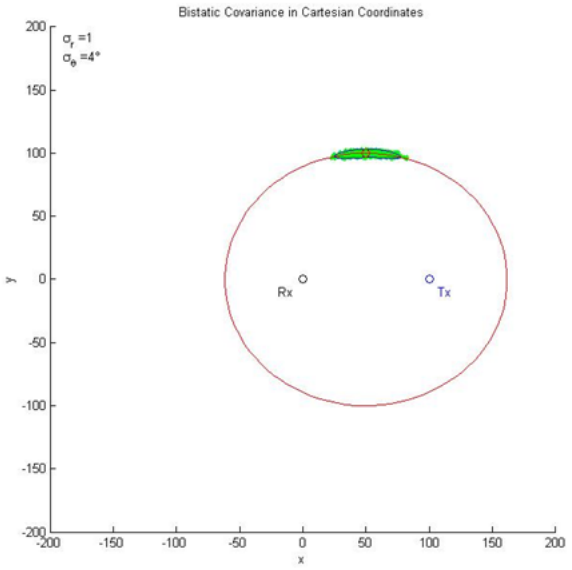

Fig. 3. Illustration of the bistatic errors for the two dimensional case, showing that they "hug" the bistatic ellipse. The measurements in this figure were generated using Gaussian measurement errors corresponding to $\sigma_b = 1$ m and $\sigma_\theta = 4°$.

is, the transformation is biased. In order to remove the biases, we must compute a first moment and second central moment that better match this distribution, which is the focus of the next section.

III. Finding the Biases

In [3], it is found that in the monostatic case for the standard conversion, i.e. for two dimensions:

$$x_m = r_m \cos\theta_m$$
$$y_m = r_m \sin\theta_m$$

given that r_m is the measured range and θ_m is the measured sensor azimuth such that

$$r_m = r + w_r$$
$$\theta_m = \theta + w_\theta$$

where w_r and w_θ represent additive white noise, the bias as a result of the conversion is *multiplicative* [7]. While it would

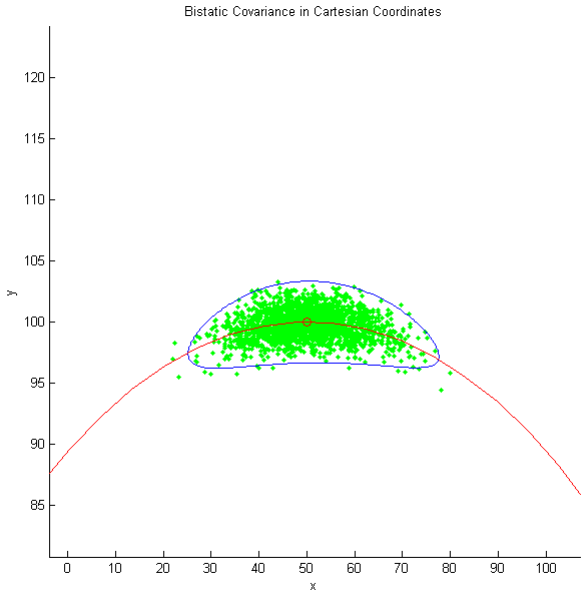

Fig. 4. Zoomed-in version of Figure 3, further illustrating how the containment region bends along the contour of constant bistatic range.

be convenient for the bistatic version of these transformations to also have multiplicative biases, this is not the case for two reasons. The first reason is that the *r-u-v* coordinate system does not in fact have a closed form for the biases [8]. The second reason is made clear by observing the expression for the receiver range R_R: the angle position and the range are coupled in the bistatic case, and hence the transformation does not have separable terms as is the case for the monostatic standard conversion. Therefore, we need to make approximations.

In order to tease out the nonlinearities in the bistatic transform, we follow a similar methodology as in [1]. However, we will find that one key difference from that work is the fact that the bias is not concentrated in the range direction. First, we define the measurements of range and angle position to be similar to the measurements in the monostatic case:

$$R_{b,m} = R_b + w_b \tag{7}$$
$$u_m = u + w_u \tag{8}$$
$$v_m = v + w_v \tag{9}$$

where

$$w_b \sim \mathcal{N}(0, \sigma_b^2) \tag{10}$$
$$w_u \sim \mathcal{N}(0, \sigma_u^2) \tag{11}$$
$$w_v \sim \mathcal{N}(0, \sigma_v^2) \tag{12}$$

That is, measurements are considered to be the true position perturbed by zero-mean, Gaussian white noise. We then define the coordinate transformations in terms of the following

functions:

$$f_x(R_b, u, v) \triangleq R_R(R_b, u, v) \cdot u \tag{13}$$

$$f_y(R_b, u, v) \triangleq R_R(R_b, u, v) \cdot v \tag{14}$$

$$f_z(R_b, u, v) \triangleq R_R(R_b, u, v) \cdot w \tag{15}$$

where the reciever range R_R is a function of R_b, u, and v and defined in terms of the intermediate variables given in Section II. The function notation for R_R will be dropped in the following expressions to make them simpler. We also make the assumption that in a Taylor expansion of the transformation equations, all terms of *third order and above* are negligible.

Using a second order Taylor series expansion of each of the transformation equations about the true position and taking the expected value of these expansions gives us the expected value of the measurements. This yields the following expressions:

$$E[x_m] \approx R_R u + \frac{1}{2}\sigma_b^2 \frac{\partial^2 f_x}{\partial R_b^2} + \frac{1}{2}\sigma_u^2 \frac{\partial^2 f_x}{\partial u^2} \tag{16}$$

$$E[y_m] \approx R_R v + \frac{1}{2}\sigma_b^2 \frac{\partial^2 f_y}{\partial R_b^2} + \frac{1}{2}\sigma_v^2 \frac{\partial^2 f_y}{\partial v^2} \tag{17}$$

$$E[z_m] \approx R_R w + \frac{1}{2}\sigma_b^2 \frac{\partial^2 f_z}{\partial R_b^2} + \frac{1}{2}\sigma_u^2 \frac{\partial^2 f_z}{\partial u^2} + \frac{1}{2}\sigma_v^2 \frac{\partial^2 f_z}{\partial v^2} \tag{18}$$

where

$$\frac{\partial^2 f_x}{\partial R_b^2} = \frac{\partial^2 R_R}{\partial R_b^2} u \tag{19}$$

$$\frac{\partial^2 f_y}{\partial R_b^2} = \frac{\partial^2 R_R}{\partial R_b^2} v \tag{20}$$

$$\frac{\partial^2 f_z}{\partial R_b^2} = \frac{\partial^2 R_R}{\partial R_b^2} w \tag{21}$$

$$\frac{\partial^2 f_x}{\partial u^2} = \frac{\partial^2 R_R}{\partial u^2} u + 2\frac{\partial R_R}{\partial u} \tag{22}$$

$$\frac{\partial^2 f_z}{\partial u^2} = w\frac{\partial^2 R_R}{\partial u^2} - 2\frac{u}{w}\frac{\partial R_R}{\partial u} - \frac{R_R}{w} - R_R\frac{u^2}{w^3} \tag{23}$$

$$\frac{\partial^2 f_y}{\partial v^2} = \frac{\partial^2 R_R}{\partial v^2} v + 2\frac{\partial R_R}{\partial v} \tag{24}$$

$$\frac{\partial^2 f_z}{\partial v^2} = w\frac{\partial^2 R_R}{\partial v^2} - 2\frac{v}{w}\frac{\partial R_R}{\partial v} - \frac{R_R}{w} - R_R\frac{v^2}{w^3} \tag{25}$$

The nonlinearities may be subtracted from the transformed coordinates in order to remove them. Neglecting the second derivatives of the receiver range with respect to the bistatic range[3], a partial evaluation of the derivatives and substitution gives the complete bias corrections.

$$c_x \approx \frac{1}{2}\sigma_u^2 \left(\frac{\partial^2 R_R}{\partial u^2} u + 2\frac{\partial R_R}{\partial u} \right) \tag{26}$$

$$c_y \approx \frac{1}{2}\sigma_v^2 \left(\frac{\partial^2 R_R}{\partial v^2} v + 2\frac{\partial R_R}{\partial v} \right) \tag{27}$$

$$\begin{aligned} c_z \approx{}& \frac{1}{2}\sigma_u^2 \left(\frac{\partial^2 R_R}{\partial u^2} w - \frac{R_R}{w} - R_R\frac{u^2}{w^3} - 2\frac{u}{w}\frac{\partial R_R}{\partial u} \right) \\ &+ \frac{1}{2}\sigma_v^2 \left(\frac{\partial^2 R_R}{\partial v^2} w - \frac{R_R}{w} - R_R\frac{v^2}{w^3} - 2\frac{v}{w}\frac{\partial R_R}{\partial v} \right) \end{aligned} \tag{28}$$

[3]When these are evaluated numerically, the results are small, within 10^{-9}.

For these expressions, the derivatives of the reciever range R_R are given by

$$\frac{\partial R_R}{\partial R_b} = \frac{0.5L_{tx} + R_b(R_b + a)}{L_m} - \frac{R_b(R_b + a)L_{tx}}{L_m^2} \tag{29}$$

$$\begin{aligned} \frac{\partial^2 R_R}{\partial R_b^2} ={}& \frac{(L_m - L_{tx})(3R_b + a) - 4R_b^2(R_b + a)}{L_m^2} \\ &+ \frac{2R_b + a}{L_m} + \frac{4R_b^2(R_b + a)L_{tx}}{L_m^3} \end{aligned} \tag{30}$$

$$\frac{\partial R_R}{\partial u} = L_{tx}\left(x_{tx} - \frac{uz_{tx}}{w}\right)\left(\frac{1}{2L_m} + \frac{a(R_b + a)}{L_m^2}\right) \tag{31}$$

$$\begin{aligned} \frac{\partial^2 R_R}{\partial u^2} = L_{tx}\Bigg[&\left(-z_{tx}\frac{w^2 + u^2}{w^3}\right)\left(\frac{1}{2L_m} + \frac{a(R_b + a)}{L_m^2}\right) \\ &+ \left(x_{tx} - \frac{uz_{tx}}{w}\right)^2 \left(\frac{R_b + 3a}{L_m^2} + \frac{4a^2(R_b + a)}{L_m^3}\right)\Bigg] \end{aligned} \tag{32}$$

$$\frac{\partial R_R}{\partial v} = L_{tx}\left(y_{tx} - \frac{vz_{tx}}{w}\right)\left(\frac{1}{2L_m} + \frac{a(R_b + a)}{L_m^2}\right) \tag{33}$$

$$\begin{aligned} \frac{\partial^2 R_R}{\partial v^2} = L_{tx}\Bigg[&\left(-z_{tx}\frac{w^2 + v^2}{w^3}\right)\left(\frac{1}{2L_m} + \frac{a(R_b + a)}{L_m^2}\right) \\ &+ \left(y_{tx} - \frac{vz_{tx}}{w}\right)^2 \left(\frac{R_b + 3a}{L_m^2} + \frac{4a^2(R_b + a)}{L_m^3}\right)\Bigg] \end{aligned} \tag{34}$$

where L_{tx} is defined to be $R_b^2 - \|\mathbf{x_{tx}}\|^2$ and L_m is defined to be $R_b^2 - a^2$.

We can see a strong dependence on the receiver range in the three bias correction terms c_x, c_y, and c_z, which should not be surprising. Once the biases are subtracted from the measurements, we can see that the expected value of the measurements becomes the true measurement value:

$$E[x_m] \approx x \tag{35}$$

$$E[y_m] \approx y \tag{36}$$

$$E[z_m] \approx z \tag{37}$$

We must now consider the change in measurement error as a result of removing the biases; i.e. derive the modified measurement covariance matrix for the transformed measurements. This is done by taking the variance of the measured Cartesian coordinates with respect to the measurements with all noise subtracted, which should be noted is *not* the same as the covariance given the true converted value. Thus, the entries in the matrix are given by the following expressions, with

non-range terms in the covariance of x_m and y_m neglected:

$$\mathrm{var}(x_m) \approx \left(\frac{\partial f_x}{\partial R_b}\right)^2 \sigma_b^2 + \left(\frac{\partial f_x}{\partial u}\right)^2 \sigma_u^2 + \frac{1}{4}\left(\frac{\partial^2 f_x}{\partial u^2}\right)^2 \sigma_u^4 \tag{38}$$

$$\mathrm{var}(y_m) \approx \left(\frac{\partial f_y}{\partial R_b}\right)^2 \sigma_b^2 + \left(\frac{\partial f_y}{\partial v}\right)^2 \sigma_v^2 + \frac{1}{4}\left(\frac{\partial^2 f_y}{\partial v^2}\right)^2 \sigma_v^4 \tag{39}$$

$$\begin{aligned}\mathrm{var}(z_m) \approx{}& \left(\frac{\partial f_z}{\partial R_b}\right)^2 \sigma_b^2 + \frac{1}{4}\left(\frac{\partial^2 f_z}{\partial R_b^2}\right)^2 \sigma_b^4 \\ &+ \left(\frac{\partial f_z}{\partial u}\right)^2 \sigma_u^2 + \frac{1}{4}\left(\frac{\partial^2 f_z}{\partial u^2}\right)^2 \sigma_u^4 \\ &+ \left(\frac{\partial f_z}{\partial v}\right)^2 \sigma_v^2 + \frac{1}{4}\left(\frac{\partial^2 f_z}{\partial v^2}\right)^2 \sigma_v^4 \\ &+ \left(\frac{\partial^2 f_z}{\partial R_b \partial u}\right)^2 \sigma_b^2\sigma_u^2 + \left(\frac{\partial^2 f_z}{\partial R_b \partial v}\right)^2 \sigma_b^2\sigma_v^2 \\ &+ \left(\frac{\partial^2 f_z}{\partial u \partial v}\right)^2 \sigma_u^2\sigma_v^2\end{aligned} \tag{40}$$

$$\mathrm{cov}(x_m, y_m) \approx \frac{\partial f_x}{\partial R_b}\frac{\partial f_y}{\partial R_b}\sigma_b^2 \tag{41}$$

$$\begin{aligned}\mathrm{cov}(x_m, z_m) \approx{}& \frac{\partial f_x}{\partial R_b}\frac{\partial f_z}{\partial R_b}\sigma_b^2 + \frac{\partial f_x}{\partial u}\frac{\partial f_z}{\partial u}\sigma_u^2 \\ &+ \frac{1}{4}\frac{\partial^2 f_x}{\partial R_b^2}\frac{\partial^2 f_z}{\partial R_b^2}\sigma_b^4 + \frac{1}{4}\frac{\partial^2 f_x}{\partial u^2}\frac{\partial^2 f_z}{\partial u^2}\sigma_u^4 \\ &+ \frac{\partial^2 f_x}{\partial R_b \partial u}\frac{\partial^2 f_z}{\partial R_b \partial u}\sigma_b^2\sigma_u^2\end{aligned} \tag{42}$$

$$\begin{aligned}\mathrm{cov}(y_m, z_m) \approx{}& \frac{\partial f_y}{\partial R_b}\frac{\partial f_z}{\partial R_b}\sigma_b^2 + \frac{\partial f_y}{\partial v}\frac{\partial f_z}{\partial v}\sigma_v^2 \\ &+ \frac{1}{4}\frac{\partial^2 f_y}{\partial R_b^2}\frac{\partial^2 f_z}{\partial R_b^2}\sigma_b^4 + \frac{1}{4}\frac{\partial^2 f_y}{\partial v^2}\frac{\partial^2 f_z}{\partial v^2}\sigma_v^4 \\ &+ \frac{\partial^2 f_y}{\partial R_b \partial v}\frac{\partial^2 f_z}{\partial R_b \partial v}\sigma_b^2\sigma_v^2\end{aligned} \tag{43}$$

(44)

For illustrative purposes, we do not expand the partials further. As we will see in further detail in the next section, this resulting covariance matrix will be significantly larger in volume than the linearized covariance.

IV. Simulation

In order to study the effects of debiasing these bistatic measurements, we first examine the purely two-dimensional case. That is, $v = 0$ in all of these simulations. We performed numerical simulations of a target moving from $(x, y) = (25\ \mathrm{km}, 100\ \mathrm{km})$ to $(25\ \mathrm{km}, -100\ \mathrm{km})$, toward a bistatic pair. The receiving radar is located at $(x_{rx}, y_{rx}) = (0\ \mathrm{m}, 0\ \mathrm{m})$, and the transmitting radar located at $(x_{tx}, y_{tx}) = (50\ \mathrm{km}, 0\ \mathrm{km})$. We assume that the target remains on boresight with respect to the receiving radar.

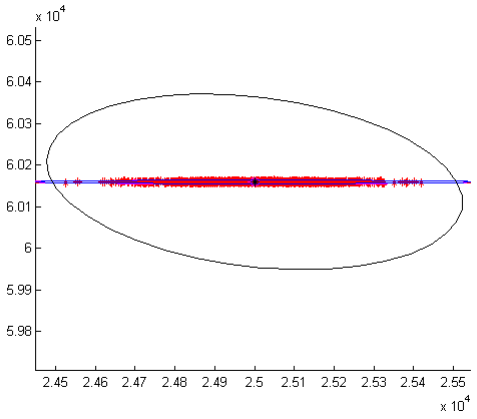

Fig. 5. Linearized (blue) and unbiased (black) covariance ellipses for $\sigma_b = 1$ m.

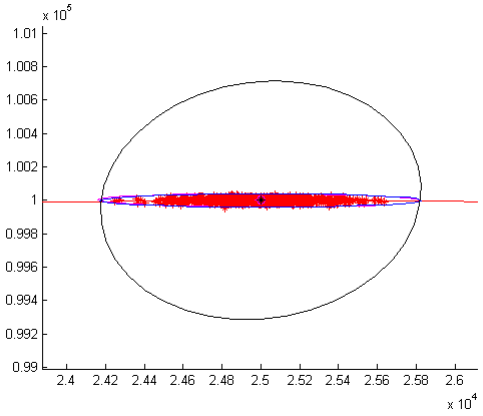

Fig. 6. Similar illustration as that of Figure 1, except $\sigma_b = 10$ m.

We then vary the sensor errors such that we see the bias effects in the measurements, and thus also observe the effects of removing the biases. The plots given in Figures 5 and 6 show the results for two values of σ_b, 1 m and 10 m. $\sigma_u = 2$ msin, in this case. We can see that in the 1 m case, the linearized covariance does not adequately cover the errors. The reason for this is that the linearized covariance, appearing to be a thick blue line in Figure 5 is tangential to the bistatic ellipse. This cannot fully cover an error volume that bends with the bistatic ellipse. Once the measurement covariance is inflated by using the equations given in Section III, the errors are effectively covered. On the other hand, for Figure 6, the linearized covariance fully covers the errors regardless of the fact that it does not hug the bistatic ellipse, which indicates that it is unnecessary to inflate the covariance to compensate.

If we look closer at these plots, as in Figures 7 and 8, we can see how debiasing affects the measurements. For clarity, we only move the sample mean, which is represented by the cross on these plots.

We can see that after debiasing, in both cases, the sample mean is situated directly over the target position, represented by the circle. If we move all of the measurements, this would place the target in the general region where the sample mean

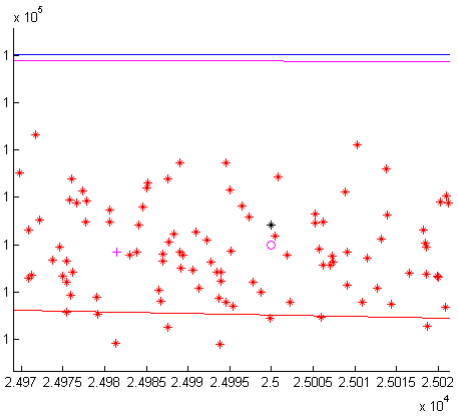

Fig. 7. Zoomed in illustration of debiased measurements. The circle is the target, the cross is the sample mean of the measurements surrounding the target, and the black star is the moved mean. $\sigma_b = 1$ m.

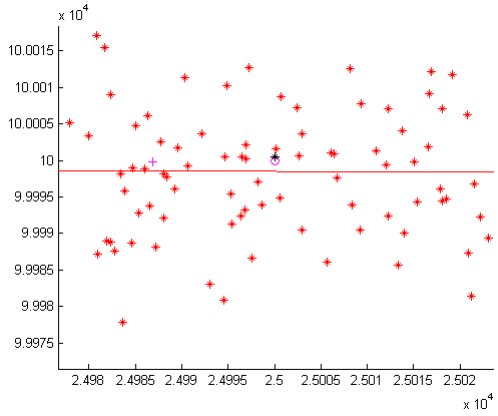

Fig. 8. Similar illustration as that of Figure 7, except $\sigma_b = 10$ m.

lies, which is the "correct" place for the target to be in relation to its measurements.

We then check statistical consistency of the unbiased covariance by calculating the normalized error squared (NES) [7] and comparing the resulting values with the biased covariance and the untransformed covariance over an interval of differing values for range error. In this case, we draw three dimensional vectors; this results in the expected value of the NES to be three. We use a 99% acceptance region for the statistic. Figure 9 shows results for one particular case. What we find is that, no, the unbiased covariance is not statistically consistent according to this test; the values do not even fall within the confidence region, which are shown by the black dotted lines. Like the biased case, the NES grows in magnitude, but not at the same rate. While the pessimism indicative of these values of the NES allows for complete containment of the errors, a smaller error volume would be more desirable. Finding ways of reducing the volume is an area of future research.

V. Conclusion

We have presented a derivation for the biases resulting from the bistatic version of the *r-u-v* conversion, as well as the means by which said biases can be removed and a demonstration of the coverage of the errors by the resulting covariance. Future work includes better characterization of the statistical consistency of the modified covariance as well as improving the consistency, and investigating better ways of performing the inflation and when to inflate, since the equations provided here overcompensate for errors when the range resolution is low. Also, algorithms that are usable on sensors of differing resolutions would require methods of switching between different measurement covariances.

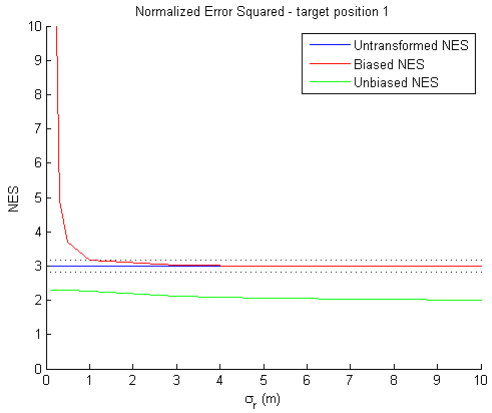

Fig. 9. Example of Normalized Error Squared (NES) for an untransformed covariance, the transformed/biased covariance, and the unbiased covariance.

References

[1] X. Tian and Y. Bar-Shalom, "Coordinate conversion and tracking for very long range radars," *IEEE Transactions on Aerospace and Electronic Systems*, vol. 45, no. 3, pp. 1073–1088, Jul 2009.

[2] D. Lerro and Y. Bar-Shalom, "Tracking with debiased consistent converted measurements versus EKF," *IEEE Transactions on Aerospace and Electronic Systems*, vol. 29, no. 3, pp. 1015–1022, Jul 1993.

[3] L. Mo, X. Song, Y. Zhou, Z. K. Sun, and Y. Bar-Shalom, "Unbiased converted measurements for tracking," *IEEE Transactions on Aerospace and Electronic Systems*, vol. 34, no. 3, pp. 1023–1027, Jul 1998.

[4] N. Willis, *Bistatic Radar*. SciTech Publishing, 2005.

[5] R. A. Coogle, J. D. Glass, L. D. Smith, P. Miceli, A. Register, P. West, and W. D. Blair, "A MIMO radar benchmarking environment," in *Proceedings of the 2011 IEEE Aerospace Conference*, Mar 2011, pp. 1–10.

[6] R. A. Coogle, J. D. Glass, L. D. Smith, and W. D. Blair, "Tracking with MIMO radar: A baseline solution," submitted to 2012 IEEE Aerospace Conference.

[7] Y. Bar-Shalom, X. Li, and T. Kirubarajan, *Estimation with Applications to Tracking and Navigation*. New York, NY: John Wiley & Sons, Inc., 2001.

[8] Y. Bar-Shalom, P. Willett, and X. Tian, *Tracking and Data Fusion: A Handbook of Algorithms*. Storrs, CT: YBS Publishing, 2011.